Amplitude and Phase Reconstruction of Electron Wave Packets for Probing Ultrafast Photoionization Dynamics

Kyung Taec Kim,[1,2] Dong Hyuk Ko,[1] Juyun Park,[1] Nark Nyul Choi,[3] Chul Min Kim,[2] Kenichi L. Ishikawa,[4] Jongmin Lee,[2] and Chang Hee Nam[1]

[1]*Department of Physics and Coherent X-Ray Research Center, Korea Advanced Institute of Science and Technology, Daejeon 305-701, Korea*

[2]*Advanced Photonics Research Institute, Gwangju Institute of Science and Technology, Gwangju 500-712, Korea*

[3]*School of Natural Science, Kumoh National Institute of Technology, Gumi 730-701, Korea*

[4]*Photon Science Center, Graduate School of Engineering, University of Tokyo, Tokyo 113-8656, Japan*

(Received 10 August 2011; published 29 February 2012)

Ultrafast atomic processes, such as excitation and ionization occurring on the femtosecond or shorter time scale, were explored by employing attosecond high-harmonic pulses. With the absorption of a suitable high-harmonic photon a He atom was ionized, or resonantly excited with further ionization by absorbing a number of infrared photons. The electron wave packets liberated by the two processes generated an interference containing the information on ultrafast atomic dynamics. The attosecond electron wave packet, including the phase, from the ground state was reconstructed first and, subsequently, that from the $1s3p$ state was retrieved by applying the holographic technique to the photoelectron spectra comprising the interference between the two ionization paths. The reconstructed electron wave packet revealed details of the ultrafast photoionization dynamics, such as the instantaneous two-photon ionization rate.

DOI: 10.1103/PhysRevLett.108.093001 PACS numbers: 32.80.Rm, 42.65.Ky, 78.47.J−

Atoms exposed to an intense laser field or a short wavelength light field can get ionized directly from the ground state or through some intermediate states. This photoionization process can occur on a time scale shorter than an optical cycle of the light field [1]. The ionization dynamics in a strong light field can be described by various ionization models studied over several decades [2–5]. However, direct experimental measurements of ultrafast ionization processes, showing how the ionization occurs in time, have only recently been achieved using attosecond pulses produced by high-harmonic generation [1]. However, the temporal resolution in this case was still limited by the duration of the probe pulse because the resultant ion yield was set by the convolution of the probe pulse and the ionization rate.

The ultrafast photoionization dynamics can be fully described by finding the amplitude and phase information of electron wave packets (EWPs) in the continuum. Attosecond high-harmonic pulses can initiate (pump) a photoionization process, generating a reference EWP in the continuum, or an excitation process. A subsequent laser pulse can produce (probe) the signal EWP from the excited state. The ultrafast dynamics of the photoionization process can be fully described by measuring the amplitude and phase of the EWPs, which can be called an ''interferometric pump-probe technique'' [6]. The retrieval of the amplitude and the phase information, thus, paves the way for acquiring a complete understanding of the photoionization process.

We have investigated the ultrafast photoionization dynamics of helium atoms by applying attosecond high-harmonic and femtosecond infrared (IR) laser pulses. A He atom can get ionized directly from the ground state by absorbing a high-harmonic photon of energy larger than the ionization potential. Alternatively, it can be resonantly excited to a certain state when the high-harmonic photon wavelength is properly tuned. Recently the interference of the EWPs generated from the photoionization of He has been investigated [6–9]. However, the amplitude and phase of the EWPs could not be measured. In this Letter, we demonstrate, for the first time, the complete amplitude and phase reconstruction of both EWPs for probing ultrafast photoionization dynamics. The EWP directly ionized from the ground state was reconstructed first by applying the complete reconstruction of attosecond burst (CRAB) method to the photoelectron spectra acquired with high-harmonic pulses and time-delayed laser pulses, serving as the ''reference'' [10,11]. The EWP from the $1s3p$ state, or the ''signal,'' was retrieved by applying a holographic technique to the photoelectron spectra which contained the interference between the two ionization paths. The reconstructed EWP revealed the instantaneous two-photon ionization rate from the excited state.

The interference between two coherent EWPs can be analyzed by using the principles of holography [12–14]. In analogy to an optical measurement, the interference observed in the photoelectron spectra can be described as a superposition of the two EWPs [15]:

$$|b|^2 = |b_R|^2 + |b_S|^2 + 2|b_R||b_S|\cos(\Delta\phi). \quad (1)$$

Here, b_R and b_S are the transition amplitudes for the reference and the signal EWPs, respectively, and $\Delta\phi$ is

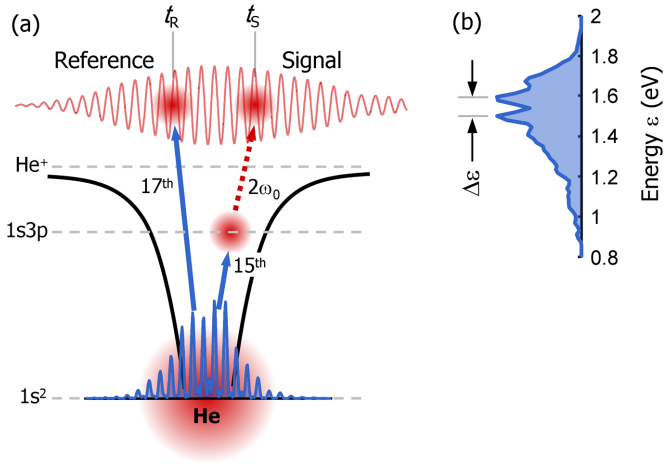

FIG. 1 (color online). (a) Illustration of the excitation and the ionization processes of He by attosecond high-harmonic pulses superposed with time-delayed IR femtosecond laser pulses. The 17th harmonic directly generates the reference wave packet from the ground state to the continuum. At the same time, the 15th harmonic can excite a ground state electron to the $1s3p$ state of He. The excited electron is, then, ionized by the probe laser pulse shown in red dotted line. (b) Photoelectron spectrum measured by applying the attosecond pulse train, generated from Ar with the laser intensity of 7×10^{14} W/cm^2, in the presence of a dressed IR laser pulse. The shown spectrum was taken with a time delay $\tau = 50$ fs.

the phase difference between the two transition amplitudes. Attosecond high-harmonic pulses were generated in an Ar gas cell by focusing 815-nm, 33-fs Ti:sapphire laser pulses with an intensity of 7×10^{14} W/cm^2 [16–18]. The reference EWP was produced by the 17th harmonic pulse as illustrated in Fig. 1(a). The signal EWP was liberated from the $1s3p$ state by a probe ir laser pulse, having an intensity of 9×10^{11} W/cm^2, with a time delay τ. The time delay "zero" was set to be the instant when the peaks of the harmonic pulse and the probe laser pulse coincided. A positive time delay means that the harmonic pulse precedes the femtosecond laser pulse. The time delay and the intensity of the probe laser pulse could be found from CRAB reconstruction results [19]. Photoelectron spectra were recorded using a magnetic-bottle time-of-flight spectrometer with a resolution of 0.025 eV at 1.6 eV [19]. Figure 1(b) shows the photoelectron spectrum generated by the combined action of the high-harmonic pulse and the femtosecond laser pulse with a time delay of 50 fs. The interference is clearly seen around the photoelectron energy of 1.6 eV, corresponding to the absorption of two IR photons by the He atom in the $1s3p$ state.

The observed interference can be understood as a spectral interference of two coherent EWPs. The delay between two EWPs can be estimated roughly from the spacing of the fringes as $\Delta\phi \approx (\varepsilon + \varepsilon_{1s3p})(t_R - t_S)$ [6]. Here, ε and ε_{1s3p} are the photoelectron energy and the binding energy of the $1s3p$ state. t_R and t_S are the ionization time of EWPs, shown in Fig. 1(a). However, the precise timing of two EWPs with respect to the probe laser pulse can be set only when the phase of the reference EWP is known. Thus, the complete description of the ultrafast ionization process requires the amplitude and phase reconstruction of both reference and signal wave packets.

For the reconstruction of EWPs, first, the reference wave packet from the ground state was retrieved. The reference EWP can be adequately described by the strong field approximation (SFA) model [10,20,21]. The transition amplitude from the ground state to the continuum state $\mathbf{p}$ in the presence of a laser field applied with a time delay τ can be written in atomic units as

$$b_R(\mathbf{p}, t \to \infty; \tau) = -i \lim_{t\to\infty} \int_{-\infty}^{t} dt' \mathbf{d}^{1s^2}_{\mathbf{p}+\mathbf{A}(t'-\tau)-\mathbf{A}(t-\tau)} \cdot \mathbf{E}_X(t') \times e^{i\phi(\mathbf{p}-\mathbf{A}(t-\tau),t'-\tau,t-\tau)} e^{i(\varepsilon+\varepsilon_{1s^2})t'}. \quad (2)$$

The dipole matrix element $\mathbf{d}^{1s^2}_{\mathbf{p}}$ can be calculated using the plane wave for the continuum state $\mathbf{p}$ and the ground state ($1s^2$) of He. $\mathbf{E}_X(t')$ is the electric field of the harmonic pulse that induces the photoionization of He. $\varepsilon = \mathbf{p}^2/2$ is the photoelectron energy, and ε_{1s^2} is the ionization potential of the ground state of He. $\mathbf{A}(t')$ is the vector potential of the laser electric field, as given by $\mathbf{E}_{\mathrm{IR}}(t') = -\partial\mathbf{A}(t')/\partial t'$. $\phi(\mathbf{p}, t' - \tau, t - \tau)$ is the temporal phase modulation that describes the free electron motion after ionization defined as [10,20,21]

$$\phi(\mathbf{p}, t', t) = -\int_{t'}^{t} dt''[\mathbf{p} \cdot \mathbf{A}(t'') + \mathbf{A}(t'')^2/2]. \quad (3)$$

The reference EWP can be reconstructed by applying the CRAB technique [10,19–24]. The amplitude and phase of $b_R(\mathbf{p})$ for each time delay τ can be completely characterized by applying Fourier transformations back and forth, while using the photoelectron spectra $S(\varepsilon = \mathbf{p}^2/2, \tau)$ in Fig. 2(b) as the intensity constraint of the phase retrieval algorithm. Although in the experiments angle-integrated photoelectron spectra were measured, they could be reasonably well approximated to the spectra emitted along the laser polarization direction [7,19]. The photoelectron spectra obtained in our measurements, however, contained the contribution from the $1s3p$ state at the energy range of the 17th harmonic, as shown in Fig. 2(a). As the contribution from excited states is not included in the SFA model, a special care was taken in the reconstruction of the reference wave packet.

The reconstruction of the reference wave packet by the CRAB method was performed with an appropriate modification. The CRAB analysis could be implemented using the photoelectron spectra without the portion of the signal wave packet [the red box in Fig. 2(b)], because all necessary information on the photoelectrons generated by the 17th harmonic was contained in the sideband appearing between those generated by the 17th and 19th harmonics.

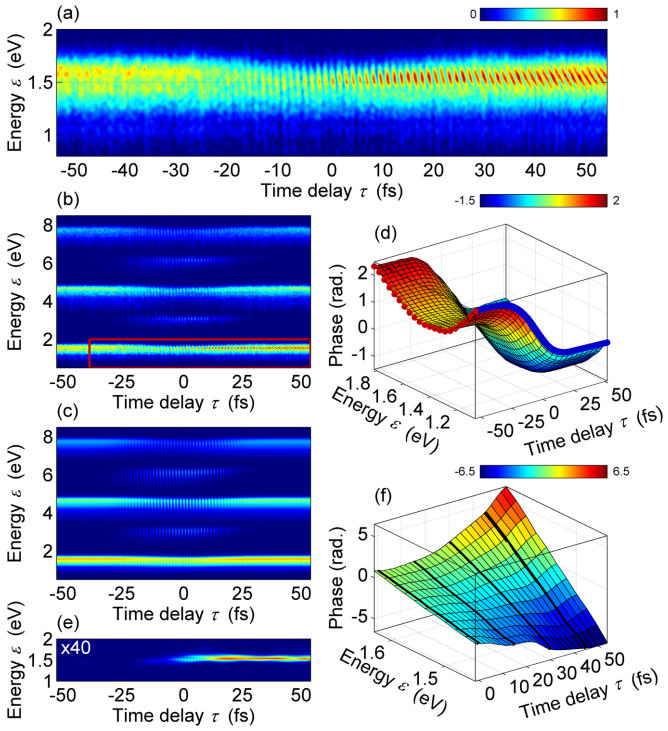

FIG. 2 (color online). Holographic reconstruction of the two EWPs liberated from the ground state and the $1s3p$ state of He. (a) Photoelectron spectra generated by high-harmonic and time-delayed IR laser pulses. Photoelectrons corresponding to the energy range of the 17th harmonic are shown. (b) Photoelectron spectra obtained in the experiment. The photoelectron peaks at 1.6, 4.7, and 7.8 eV represent the photoelectron produced by 17th, 19th, and 21st harmonics. (c) Reference EWP, $p|b_R(\mathbf{p})|^2$. (d) Phase of the reference EWP. (e) Signal EWPs, $p|b_S(\mathbf{p})|^2$. (f) Phase of the signal EWP, reconstructed by applying the holographic technique for the direction of the laser polarization. The phase of the signal wave packet was drawn after subtracting $2\omega_0\tau$ for better visualization. The same color code was used for the number density of photoelectrons in (a), (b), (c), and (e). The number density in (e) was multiplied by 40.

The amplitude and phase of the reference wave packet were successfully reconstructed using the partially removed photoelectron spectra, as shown in Figs. 2(c) and 2(d), respectively. It contained the information on the dynamics of the electron directly ionized from the ground state by the attosecond harmonic pulses in the presence of the laser field. Since the intensity of the driving laser pulse used for the harmonic generation was relatively high, the laser pulse became positively chirped during propagation in the ionizing medium [25], and the 17th harmonic pulse also became positively chirped [19]. The quadratic phase of the reference EWP, indicated by the red dotted line in Fig. 2(d), shows the phase inherited from the positively chirped 17th harmonic. The phase of the reference is also modulated with respect to the time delay of the laser field, as indicated by the blue solid line in Fig. 2(d). The phase of the reference wave packet changes slowly with time delay due to the $\mathbf{A}^2$ term in Eq. (3), corresponding to the ponderomotive shift. The fast oscillation term $(\mathbf{p}\cdot\mathbf{A})$ corresponds to the momentum shift due to the probe laser field, which is too small to be visible here. The reconstructed result, obtained by the CRAB analysis, accounted for the expected characteristics of the reference EWP quite well.

The signal EWP liberated from the $1s3p$ state of helium atom carries the important information about the excitation and ionization processes. Since the reference EWP was completely characterized with the phase information, the signal EWP could be obtained from the interference term in Eq. (1). The resultant amplitude and phase of the reconstructed wave packet are shown in Figs. 2(e) and 2(f), respectively. For negative time delays, as expected, no significant ionization occurs as is evident from Fig. 2(e). The amplitude of the signal EWP starts to increase from around $\tau = 0$, i.e., the instant when the laser pulse overlaps with the harmonic pulse. The measured bandwidth of the signal wave packet in Fig. 2(a) is about 0.14 and 0.10 eV, respectively, for $\tau = 0$ and 30 fs. As a narrower bandwidth of the wave packet means a longer temporal profile in the time domain, the ionization occurs for a longer duration for the larger time delay. The reconstructed phase of the signal EWP, shown in Fig. 2(f), also provides the timing information. The slope of the phase, $t_S = \partial\varphi_S/\partial\varepsilon$, is the group delay of the signal wave packet, from which the time of ionization may be obtained. The group delays were directly calculated to be 8.6, 13, 24, and 38 fs, respectively, for the time delays of 0, 15, 30, and 45 fs. This result indicates that for $\tau = 0$ the ionization peaked 8.6 fs after the excitation by the harmonic pulse, but for $\tau = 15$ fs it was delayed further by only 4.4 fs. When the probe laser pulse followed the harmonic pulse without any overlap, the group delay increased almost linearly with time delay. Although the duration and the time of ionization peak could be obtained from the reconstructed amplitude and phase, a more rigorous analysis was performed to understand the detailed ionization dynamics.

The temporal profile of the ionization process can be obtained by modeling the ionization process in accordance with the SFA model. The transition amplitude of the signal wave packet, liberated from the $1s3p$ state by the probe laser field applied after a time delay τ, can be described as [26,27],

$$b_S(\mathbf{p},t;\tau) = -i\int_{-\infty}^{t} dt' a_{1s3p}(t';\tau) \times \mathbf{d}^{1s3p}_{\mathbf{p}+\mathbf{A}(t'-\tau)-\mathbf{A}(t-\tau)}\cdot\mathbf{E}_{\mathrm{IR}}(t'-\tau) \times e^{i\phi(\mathbf{p}-\mathbf{A}(t-\tau),t'-\tau,t-\tau)}e^{i(\varepsilon+\varepsilon_{1s3p})t'}. \quad (4)$$

The complex amplitude of the $1s3p$ state can be expressed as $a_{1s3p}(t';\tau) = |a_{1s3p}(t';\tau)|e^{i\Delta\varepsilon_{1s3p}(t';\tau)t'}$. The population of the $1s3p$ state is given by $|a_{1s3p}(t';\tau)|^2$, and $\Delta\varepsilon_{1s3p}(t';\tau)$ in the phase term is the Stark shift. The dipole matrix element $\mathbf{d}^{1s3p}_{\mathbf{p}}$ is obtained from the calculation using

the plane wave for the continuum state $\mathbf{p}$ and the wave function of the excited state ($1s3p$). The exact form of $E_{\mathrm{IR}}(t')$ and $\phi(t')$ can be obtained by the CRAB analysis using Eq. (3). Note that we already have the complete information of the signal wave packet b_s in the left-hand side of Eq. (4) for $t \to \infty$, as presented in Figs. 2(e) and 2(f). Thus, $a_{1s3p}(t';\tau)$ can be determined by taking the inverse Fourier transform of $b_S(\mathbf{p}, t \to \infty;\tau)$ and dividing by the second harmonic component of $\mathbf{d}^{1s3p}_{\mathbf{p}+\mathbf{A}(t'-\tau)-\mathbf{A}(t-\tau)} \cdot \mathbf{E}_{\mathrm{IR}}(t'-\tau)e^{i\phi(\mathbf{p}-\mathbf{A}(t-\tau),t'-\tau,t-\tau)}$ [28]. In this process, the momentum dependence could be ignored due to the narrow bandwidth of the signal. Once $a_{1s3p}(t;\tau)$ is obtained, the transition amplitude for a given time delay τ can be obtained for any time t using Eq. (4).

The retrieved transition amplitude can describe the ionization dynamics from the excited state. The number of electrons that contribute to the two-photon transition can be calculated by integrating $|b_S(\mathbf{p}, t;\tau)|^2$ in the momentum space for the momentum states that finally contribute to the two-photon transition:

$$N_{2\omega_0}(t;\tau) = \int |b_S(\mathbf{p}, t;\tau)|^2 d^3\mathbf{p}. \quad (5)$$

Figure 3 shows the instantaneous ionization rate, $dN_{2\omega_0}(t;\tau)/dt$, that describes the rate of electron liberation into the continuum. The excitation and ionization dynamics of He in the $1s3p$ state can be traced on the femtosecond time scale. For the validity confirmation of our approach based on the SFA, a whole reconstruction procedure was carried out by directly solving the time-dependent Schrödinger equation, which showed very good agreement with the current results [28]. The population of the $1s3p$ state increases due to the excitation by the 15th harmonic and decreases due to the ionization by the probe laser pulse. The population amplitude $|a_{1s3p}(t;\tau)|^2$ and the instantaneous ionization rate $dN_{2\omega_0}(t;\tau)/dt$ are shown in Fig. 3 as black dashed line and green thick solid lines, respectively. It is seen that for $\tau = 0$ the population increases while the attosecond harmonic pulse exists, indicating that the instantaneous ionization rate is much smaller than the excitation rate. The instantaneous ionization rate peaks slightly earlier than the peak of $|a_{1s3p}(t;\tau)|^2$, as the instantaneous laser intensity decreases in the trailing edge. For $\tau = 15$ fs, the instantaneous ionization rate is delayed only slightly because the laser intensity varies slowly near the peak. Since the laser intensity peaks after the peak of the excitation, the ionization lasts longer and is asymmetric. As the time delay increases further ($\tau = 30$ fs and 45 fs), the peak of the ionization is almost linearly delayed. In these cases, the overlap between the attosecond harmonic pulse and the laser pulse is minimal, and the electron stays in the $1s3p$ state until it experiences a laser field strong enough to ionize it. The duration of the ionization is longer due to low ionization rate. Thus, the two-photon ionization dynamics of the

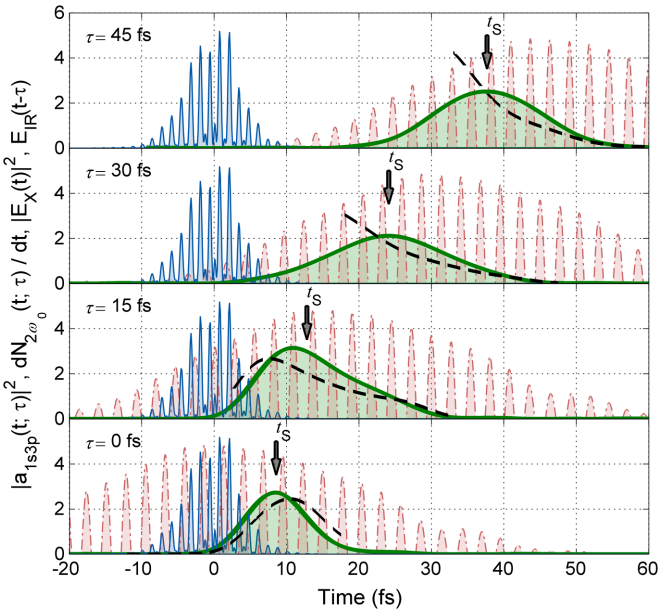

FIG. 3 (color online). Ionization dynamics of the $1s3p$ state of He. The population amplitude of the $1s3p$ state $|a_{1s3p}(t;\tau)|^2$, black dashed line, the instantaneous ionization rate for the two-photon ionization $dN_{2\omega_0}(t;\tau)/dt$, green thick solid line, the intensity profile of the attosecond pulse train $|E_X(t)|^2$, blue thin solid line, the electric field of the probe laser pulse $E_{\mathrm{IR}}(t-\tau)$, red dash-dotted line are shown for the time delays of 0, 15, 30, and 45 fs. The group delay t_S of the signal EWPs, obtained from Fig. 2(f), is indicated with an arrow for each time delay. $|a_{1s3p}(t;\tau)|^2$ is shown only for the range where the electric field is strong so that the calculation error should not be large. All quantities are in arbitrary units.

excited He state in the femtosecond laser field could be completely understood from the reconstructed population amplitude and the instantaneous ionization rate.

In summary, we have successfully reconstructed the EWPs, including the phase information, from the ground state as well as the $1s3p$ state of He and showed the excitation and ionization dynamics. The reconstructed EWPs were used to describe the excitation and ionization dynamics of He. Though the photoelectron spectra were measured only after the interaction, the reconstruction of the ionization process was achieved by tracing back the process employing the SFA model, which yielded good accuracy. Since the information on an excited quantum state can be retrieved from the reconstruction of EWPs, this technique should also be useful for understanding attosecond atomic and molecular dynamics, including those involving multiple excitation and ionization steps such as autoionization or shakeup processes.

This work was supported by the Ministry of Education, Science, and Technology of Korea through the National Research Foundation, and by the Ultrashort Quantum Beam Facility Program of the Ministry of Knowledge Economy of Korea. K. L. I. gratefully acknowledges the

support by the Advanced Photon Science Alliance project of the Ministry of Education, Culture, Sports, Science and Technology of Japan, and KAKENHI (23656043 and 23104708).

[1] M. Uiberacker *et al.*, Nature (London) **446**, 627 (2007).
[2] M. V. Ammosov, N. B. Delone, and V. P. Krainov, Sov. Phys. JETP **64**, 1191 (1986).
[3] A. M. Perelemov, V. S. Popov, and M. V. Terent'ev, Sov. Phys. JETP **23**, 924 (1966).
[4] H. R. Reiss, Phys. Rev. A **22**, 1786 (1980).
[5] G. L. Yudin and M. Y. Ivanov, Phys. Rev. A **64**, 013409 (2001).
[6] J. Mauritsson *et al.*, Phys. Rev. Lett. **105**, 053001 (2010).
[7] P. Johnsson, J. Mauritsson, T. Remetter, A. L'Huillier, and K. J. Schafer, Phys. Rev. Lett. **99**, 233001 (2007).
[8] M. Swoboda *et al.*, Phys. Rev. Lett. **104**, 103003 (2010).
[9] M. Holler, F. Schapper, L. Gallmann, and U. Keller, Phys. Rev. Lett. **106**, 123601 (2011).
[10] Y. Mairesse and F. Quere, Phys. Rev. A **71**, 011401(R) (2005).
[11] V. S. Yakovlev, J. Gagnon, N. Karpowicz, and F. Krausz, Phys. Rev. Lett. **105**, 073001 (2010).
[12] C. Leichtle, W. P. Schleich, I. Sh. Averbukh, and M. Shapiro, Phys. Rev. Lett. **80**, 1418 (1998).
[13] T. C. Weinacht, J. Ahn, and P. H. Bucksbaum, Nature (London) **397**, 233 (1999).
[14] T. C. Weinacht, J. Ahn, and P. H. Bucksbaum, Phys. Rev. Lett. **80**, 5508 (1998).
[15] M. Wollenhaupt, A. Assion, D. Liese, Ch. Sarpe-Tudoran, T. Baumert, S. Zamith, M. A. Bouchene, B. Girard, A. Flettner, U. Weichmann, and G. Gerber, Phys. Rev. Lett. **89**, 173001 (2002).
[16] K. T. Kim, C. M. Kim, M. -G. Baik, G. Umesh, and C. H. Nam, Phys. Rev. A **69**, 051805(R) (2004).
[17] D. G. Lee, J. J. Park, J. H. Sung, and C. H. Nam, Opt. Lett. **28**, 480 (2003).
[18] H. T. Kim *et al.*, Phys. Rev. A **67**, 051801(R) (2003).
[19] K. T. Kim, D. H. Ko, J. J. Park, V. Tosa, and C. H. Nam, New J. Phys. **12**, 083019 (2010).
[20] F. Quere, Y. Mairesse, and J. Itatani, J. Mod. Opt. **52**, 339 (2005).
[21] M. Kitzler, N. Milosevic, A. Scrinzi, F. Krausz, and T. Brabec, Phys. Rev. Lett. **88**, 173904 (2002).
[22] H. Wang *et al.*, J. Phys. B **42**, 134007 (2009).
[23] J. Gagnon, E. Goulielmakis, and V. S. Yakovlev, Appl. Phys. B **92**, 25 (2008).
[24] D. J. Kane, IEEE J. Quantum Electron. **35**, 421 (1999).
[25] H. J. Shin, D. G. Lee, Y. H. Cha, K. H. Hong, and C. H. Nam, Phys. Rev. Lett. **83**, 2544 (1999).
[26] M. Lewenstein, Ph. Balcou, M. Y. Ivanov, A. L'Huillier, and P. B. Corkum, Phys. Rev. A **49**, 2117 (1994).
[27] M. Wickenhauser, X. M. Tong, and C. D. Lin, Phys. Rev. A **73**, 011401(R) (2006).
[28] See Supplemental Material at http://link.aps.org/supplemental/10.1103/PhysRevLett.108.093001 for the detailed reconstruction procedure tested using the photoelectron spectra calculated by solving TDSE model.